Three LysM effectors of Zymoseptoria tritici collectively disarm chitin-triggered plant immunity

SCHOLARONE™
Manuscripts

1 # Three LysM effectors of *Zymoseptoria tritici* collectively

2 # disarm chitin-triggered plant immunity

3

4 **Hui Tian[1,2], Craig I. MacKenzie[1,‡], Luis Rodriguez-Moreno[1,#,‡], Grardy C.M. van den**

5 **Berg[1], Hongxin Chen[3], Jason J. Rudd[3], Jeroen R. Mesters[4], Bart P.H.J. Thomma[1,2,*]**

6

7 [1]Laboratory of Phytopathology, Wageningen University and Research,

8 Droevendaalsesteeg 1, 6708PB Wageningen, The Netherlands

9 [2]University of Cologne, Institute for Plant Sciences, Cluster of Excellence on Plant

10 Sciences (CEPLAS), 50674 Cologne, Germany.

11 [3]Department of Bio-Interactions and Crop Protection, Rothamsted Research, Harpenden,

12 AL5 2JQ, UK

13 [4]Institute of Biochemistry, University of Lübeck, Ratzeburger Allee 160, 23538 Lübeck,

14 Germany

15

16 Present address:

17 [#]Departamento de Biología Celular, Genética y Fisiología, Universidad de Málaga,

18 Málaga, Spain

19

20 [‡]These authors contributed equally

21 [*]To whom correspondence should be addressed. E-mail: bthomma@uni-koeln.de

SUMMARY

Chitin is a major structural component of fungal cell walls and acts as a microbe-associated molecular pattern (MAMP) that, upon recognition by a plant host, triggers the activation of immune responses. In order to avoid the activation of these responses, the Septoria tritici blotch (STB) pathogen of wheat, *Zymoseptoria tritici*, secretes LysM effector proteins. Previously, the LysM effectors Mg1LysM and Mg3LysM were shown to protect fungal hyphae against host chitinases. Furthermore, Mg3LysM, but not Mg1LysM, was shown to suppress chitin-induced reactive oxygen species (ROS) production. Whereas initially a third LysM effector gene was disregarded as a presumed pseudogene, we now provide functional data to show that also this gene encodes a LysM effector, named Mgx1LysM, that is functional during wheat colonization. While Mg3LysM confers a major contribution to *Z. tritici* virulence, Mgx1LysM and Mg1LysM contribute to *Z. tritici* virulence with smaller effects. All three LysM effectors display partial functional redundancy. We furthermore demonstrate that Mgx1LysM binds chitin, suppresses the chitin-induced ROS burst and is able to protect fungal hyphae against chitinase hydrolysis. Finally, we demonstrate that Mgx1LysM is able to undergo chitin-induced polymerisation. Collectively, our data show that *Zymoseptoria tritici* utilizes three LysM effectors to disarm chitin-triggered wheat immunity.

INTRODUCTION

Plants deploy an effective innate immune system to recognize and appropriately respond to microbial invaders. An important part of this immune system involves the recognition of conserved microbe-associated molecular patterns (MAMPs) that are recognized by cell surface-localized pattern recognition receptors (PRRs) to activate pattern-triggered immunity (PTI) (Cook *et al.*, 2015; Jones and Dangl, 2006; Thomma *et al.*, 2001). PTI includes a broad range of immune responses, such as the production of reactive oxygen species (ROS), ion fluxes, callose deposition and defence-related gene expression (Altenbach and Robatzek, 2007; Boller and Felix, 2009; Jones and Dangl, 2006).

Chitin, a homopolymer of β-(1,4)-linked *N*-acetylglucosamine (GlcNAc), is an abundant polysaccharide in nature and a major structural component of fungal cell walls (Free, 2013). Plants secrete hydrolytic enzymes, such as chitinases, as an immune response to target fungal cell wall chitin in order to disrupt cell wall integrity, and also to release chitin molecules that act as a MAMP that can be recognized by PRRs that carry extracellular lysin motifs (LysMs) to activate further immune responses against fungal invasion (Felix *et al.*, 1993; Kombrink and Thomma, 2013; Sánchez-Vallet *et al.*, 2015). To date, chitin receptor complexes that comprise LysM-containing receptors have been characterized in Arabidopsis and rice (Cao *et al.*, 2014; Miya *et al.*, 2007; Shimizu *et al.*, 2010; Wan *et al.*, 2012). Homologs of the crucial components of these complexes have also been identified in wheat (Lee *et al.*, 2014).

In order to successfully establish an infection, fungal pathogens evolved various strategies to overcome chitin-triggered plant immunity, such as alternation of cell wall chitin in such way that it is no longer recognized (Fujikawa *et al.*, 2009; Fujikawa *et al.*, 2012), but also the secretion of effector proteins to either protect fungal cell walls against hydrolytic host enzymes or to prevent the activation of chitin-induced immunity (van den

Burg *et al.*, 2006; Kombrink *et al.*, 2011; Marshall *et al.*, 2011; Mentlak *et al.*, 2012;

Rovenich *et al.*, 2014; Takahara *et al.*, 2016). For example, some fungi can convert the

surface-exposed chitin in fungal cell walls to chitosan, which is a poor substrate for

chitinases, thus avoiding the activation of chitin-triggered immune responses during host

invasion (El Gueddari *et al.*, 2002; Ride and Barber, 1990). Furthermore, from the soil-

borne fungus *Verticillium dahliae* a secreted polysaccharide deacetylase was

characterized to facilitate fungal virulence through direct deacetylation of chitin

oligomers, converting them to chitosan (Gao *et al.*, 2019). The use of effector molecules to

successfully target chitin-triggered plant immunity has been well-studied for the tomato

leaf mould fungus *Cladosporium fulvum*. This fungus secretes the invertebrate chitin-

binding domain (CBM14)-containing effector protein Avr4 to bind fungal cell wall chitin,

resulting in the protection of its hyphae against hydrolysis by tomato chitinases (van den

Burg *et al.*, 2006; van Esse *et al.*, 2007). Additionally, *C. fulvum* secretes the effector protein

Ecp6 (extracellular protein 6) that carries three LysMs, binds chitin and suppresses

chitin-induced plant immunity. A crystal structure of Ecp6 revealed that two of its three

LysM domains undergo ligand-induced intramolecular dimerization, thus establishing a

groove with ultrahigh (pM) chitin binding-affinity that enables Ecp6 to outcompete plant

receptors for chitin binding (Sánchez-Vallet *et al.*, 2013). Therefore, Avr4 and Ecp6 have

complementary activities, where Avr4 protects hyphae but does not suppress chitin-

triggered immunity, and Ecp6 suppresses chitin-triggered immunity but does not protect

hyphae (Bolton *et al.*, 2008; de Jonge *et al.*, 2010). Homologs of Ecp6, coined LysM

effectors, have been found in many fungi (de Jonge and Thomma, 2009) and include the

functionally analysed *Magnaporthe oxyzae* Slp1, *Colletotrichum higginsianum* Elp1 and

Elp2, *Verticillium dahliae* Vd2LysM, *Rhizoctonia solani* RsLysM and LysM1 and LysM2

from the mycoparasitic fungus *Clonostachys rosea* (Dolfors *et al.*, 2019; Dubey *et al.*, 2020;

90   Kombrink *et al.*, 2017; Mentlak *et al.*, 2012; Takahara *et al.*, 2016). In contrast, homologs

91   of Avr4 are less widespread (Stergiopoulos *et al.*, 2010).

92   *Zymoseptoria tritici* (formerly *Mycosphaerella graminicola*) is a host-specific

93   hemibiotrophic fungus and the causal agent of Septoria tritici blotch (STB) of wheat

94   (*Triticum* spp.) (Eyal, 1999). Upon infection, wheat plants undergo an extended period of

95   symptomless colonization of approximately one week, followed by the death of host

96   tissues coinciding with rapid invasive growth and asexual reproduction of the fungus

97   (Glazebrook, 2005; Kema *et al.*, 1996; Pnini-Cohen *et al.*, 2000). This transition from

98   biotrophic to necrotrophic growth of *Z. tritici* is associated with the induction of host

99   immune processes such as a hypersensitive response (HR)-like programmed cell death

100   and differential expression of wheat mitogen-activated protein kinase (MAPK) genes

101   (Rudd *et al.*, 2008). Three LysM effector genes were previously identified in the *Z. tritici*

102   genome (Marshall *et al.*, 2011). These comprise *Mg1LysM* and *MgxLysM* that encode LysM

103   effector proteins that carry a single LysM only, and *Mg3LysM* encoding an effector with

104   three LysMs (Marshall *et al.*, 2011). Whereas *Mg1LysM* and *Mg3LysM* were subjected to

105   functional analysis, *MgxLysM* was disregarded because this gene lacked expressed

106   sequence tag (EST) support and was believed to contain an intronic repeat insertion,

107   rendering it a pseudogene. Both *Mg1LysM* and *Mg3LysM* were found to be induced during

108   wheat infection, and both proteins were found to bind chitin. However, only Mg3LysM

109   was found to suppress chitin-induced plant immunity (Marshall *et al.*, 2011). Surprisingly,

110   and in contrast to Ecp6, both Mg1LysM and Mg3LysM were found to protect fungal hyphae

111   against plant chitinase activity. Recently, a crystal structure was generated and revealed

112   that Mg1LysM undergoes chitin-dependent dimerization of ligand-independent

113   homodimers, and it was proposed that chitin-induced polymerization of Mg1LysM in the

114   fungal cell wall confers protection against chitinases (Sánchez-Vallet *et al.*, 2020).

115   However, thus far the mechanism underlying the protection of cell walls by Mg3LysM

116   remains unclear. In this study, we revisit the previously discarded *MgxLysM* gene and

117   evaluate its contribution to *Z. tritici* virulence on wheat plants.

118

119   **RESULTS**

120   *Mgx1LysM* **is expressed during wheat colonization**

121   Although *MgxLysM* was previously reported to be a pseudogene and found not to be

122   induced upon wheat infection (Marshall *et al.*, 2011), a more recent transcriptome

123   profiling study on wheat demonstrated *MgxLysM* expression during host colonization,

124   demonstrating that the initial assessment was incorrect (Rudd *et al.*, 2015). Thus, we

125   propose to rename MgxLysM to Mgx1LysM, according to the single LysM domain in the

126   protein, similar to the previously described Mg1LysM effector (Marshall *et al.*, 2011).

127   To confirm the expression of *Mgx1LysM* in *Z. tritici* upon host colonization, we

128   inoculated the wild-type strain IPO323 onto wheat leaves and sampled leaves at 0, 4, 8,

129   10 and 14 days post inoculation (dpi). In addition, we subjected IPO323 growing *in vitro*

130   in Czapek-Dox broth (CDB) and in potato dextrose broth (PDB) to expression analysis. We

131   confirmed that *Mgx1LysM* is not expressed upon growth *in vitro*, but only during host

132   colonization at all tested time points (Fig. 1). More specifically, *Mgx1LysM* expression was

133   strongly induced at 4 dpi, peaked at 8 dpi and dramatically decreased by 10 dpi.

134   Interestingly, the peak of expression at 8 dpi is around the transition time when the

135   infection switches from asymptomatic to symptomatic with the appearance of lesions on

136   wheat leaves (Marshall *et al.*, 2011).

137

Mgx1LysM contributes to *Z. tritici* virulence on wheat and displays functional redundancy with Mg1LysM and Mg3LysM

Since *Mgx1LysM* is expressed by *Z. tritici* during colonization of wheat plants, we further assessed whether Mgx1LysM contributes to *Z. tritici* virulence and whether it shares functional redundancy with Mg1LysM and Mg3LysM. To this end, we generated the single-gene deletion mutant *ΔMgx1*, the double-gene deletion mutants *ΔMg1-ΔMgx1* and *ΔMgx1-ΔMg3*, and the triple-gene deletion mutant *ΔMg1-ΔMgx1-ΔMg3* in a *Δku70* mutant, which is unaltered in virulence but has improved homologous recombination frequencies (Bowler *et al.*, 2010). The absence of *Mgx1LysM* combined with the presence of the resistance marker (*NAT*) was confirmed with PCR in two independent transformants for each of the combinations (Fig. S1A). To assess the possibility of additional ectopic insertions, *NAT* copy numbers in the genomes of single-, double- and triple-gene deletion mutants were determined with real-time PCR, using *Z. tritici β-tubulin* as a single gene-copy control. As typically expected for *Agrobacterium tumefaciens*-mediated transformation, all transformants carried a single copy of the transgene, suggesting a single T-DNA insertion (Fig. S1B).

To evaluate the contribution to virulence of each of the LysM effectors, two independent *ΔMgx1*, *ΔMg1-ΔMgx1*, *ΔMgx1-ΔMg3* and *ΔMg1-ΔMgx1-ΔMg3* transformants were inoculated onto wheat plants, together with the previously tested gene deletion mutants *ΔMg1, ΔMg3* and *ΔMg1-ΔMg3* (Marshall *et al.*, 2011). All mutants were generated in the *Δku70* mutant that was used as wild-type (WT) in this study. By 21 days post inoculation (dpi), the WT strain caused typical necrosis symptoms on the wheat leaves, while *ΔMg3* strains caused much less necrotic symptoms (Fig. 2AB) as previously reported (Marshall *et al.*, 2011). Furthermore, like previously reported, plants inoculated with the *ΔMg1* strains developed similar necrosis as with the WT strain. We now show

163 not only that the *ΔMgx1* strains caused similar levels of necrosis as the WT and *ΔMg1*

164 strains, but also that the *ΔMg1-ΔMgx1* strains shows no apparent decrease in disease

165 development, suggesting that these two LysM effectors are dispensable for virulence of *Z.*

166 *tritici*. In line with these observations, both the *ΔMgx1-ΔMg3* strains and the *ΔMg1-ΔMg3*

167 strains induced similar symptoms as the *ΔMg3* strains (Fig. 2AB). Nevertheless, the

168 necrotic symptoms caused by inoculation with the *ΔMg1-ΔMgx1-ΔMg3* strains were

169 drastically reduced when compared with those caused by the *ΔMg3* strains. Collectively,

170 these findings suggest that Mg3LysM is the most important LysM effector for *Z. tritici*

171 disease development, and that Mgx1LysM and Mg1LysM contribute to disease

172 development through redundant functionality.

173   To further substantiate the fungal colonization assessments, we measured fungal

174 biomass with real-time PCR. While the *ΔMg1* and *ΔMgx1* strains developed similar

175 amounts of fungal biomass as the WT strain, *ΔMg1-ΔMgx1* strains displayed significantly

176 compromised colonization, but not as compromised as the *ΔMg3* strains or the double and

177 triple mutants that lack *Mg3LysM* (Fig. 2C). These observations confirm that the three

178 LysM effectors make differential contributions to symptom display, which is accompanied

179 by distinct differential contributions to fungal colonization. Thus, our findings present

180 evidence for partially redundant, but also partially divergent, contributions of the three

181 LysM effectors to *Z. tritici* virulence.

182

183 **LysM effectors differentially contribute to *Z. tritici* pycnidia formation on wheat**

184 Soon after the onset of necrotic symptoms, asexual fruiting bodies (pycnidia) can be

185 formed (Karisto *et al.*, 2018; Kema *et al.*, 1996). Thus, we determined the percentage of

186 leaf surface displaying pycnidia coverage at 17 dpi. Surprisingly, repeated assays revealed

187 that the *ΔMg1* strains developed significantly more pycnidia than the WT strain, whereas

188   the *ΔMgx1* strains, like the *ΔMg3* strains, produced no to only a few pycnidia (Fig. S2).

189   Accordingly, whereas the *ΔMg1-ΔMgx1* strains developed an intermediate number of

190   pycnidia, all mutants that involved *ΔMg3* were devoid of pycnidia (Fig. S2). These data

191   first of all suggest that symptom development does not correlate with fungal colonization

192   levels as measured by pycnidia formation and, furthermore, that the three LysM effectors

193   display differential roles in fungal colonization.

194

Mgx1LysM binds chitin and suppresses the chitin-induced ROS burst

196   To investigate how Mgx1LysM contributes to *Z. tritici* virulence during wheat colonization,

197   we first assessed its substrate-binding characteristics. Mgx1LysM was heterologously

198   expressed in *E. coli* and subjected to a polysaccharide precipitation assay. Mgx1LysM was

199   incubated with chitin beads and shrimp shell chitin, but also with plant-derived cellulose

200   and xylan, revealing that Mgx1LysM binds chitin beads and shrimp shell chitin but not

201   cellulose or xylan (Fig. 3). Thus, Mgx1LysM resembles Mg1LysM that similarly binds

202   chitin but not cellulose or xylan (Fig. 3).

203   To test whether Mgx1LysM can prevent chitin-triggered immunity in plants, the

204   occurrence of a chitin-induced ROS burst was assessed in *Nicotiana benthamiana* leaf

205   discs upon treatment with 10 μM chitohexaose (chitin) in the presence or absence of

206   effector protein. As previously demonstrated (de Jonge *et al.*, 2010), *C. fulvum* Ecp6

207   suppresses ROS production in this assay (Fig. 4). Remarkably, pre-incubation of 10 μM

208   chitin with 50 μM Mgx1LysM prior to the addition to leaf discs led to a significant

209   reduction of the ROS burst (Fig. 4), demonstrating its ability to suppress chitin-induced

210   plant immune responses. This finding was unexpected because we previously found that

211   its close homolog Mg1LysM cannot suppress a chitin-induced defense response in a

212   tomato cell culture (Marshall *et al.*, 2011), albeit that in that study Mg1LysM was

213 heterologously produced in the yeast *Pichia pastoris* rather than in *E. coli*. To revisit this

214 initial observation, we now test whether *E. coli*-produced Mg1LysM is able to suppress

215 the chitin-induced ROS burst. Indeed, similar to the results obtained for Mgx1LysM, we

216 observed that pre-incubation of 10 µM chitin with 50 µM Mg1LysM prior to the addition

217 to leaf discs led to a significantly compromised ROS burst. Thus, both LysM effectors can

218 suppress chitin-triggered host immunity.

219

Mgx1LysM protects hyphae against chitinases

221 We previously demonstrated that Mg1LysM can protect fungal hyphae against chitinase

222 hydrolysis (Marshall *et al.*, 2011). To evaluate a possible role in hyphal protection,

223 Mgx1LysM was tested for its ability to protect hyphae of *Trichoderma viride*, a fungus that

224 exposes its cell wall chitin *in vitro*, against chitinases was tested (Mauch *et al.*, 1988). The

225 *C. fulvum* effector protein Avr4 and Mg1LysM were used as positive controls based on

226 their previously demonstrated ability to protect fungal hyphae (van den Burg *et al.*, 2006;

227 Marshall *et al.*, 2011). As expected, while the addition of chitinase drastically inhibited *T.*

228 *viride* hyphal growth, Avr4 as well as Mg1LysM protected the hyphae against hydrolysis

229 by chitinases from *Clostridium thermocellum* (Fig. 5) as well as from tomato (Fig. S3).

230 Furthermore, Mgx1LysM similarly protected the hyphae against chitinase hydrolysis (Fig.

231 5).

232

Mgx1LysM undergoes chitin-dependent polymerization

234 Recently, Mg1LysM was demonstrated to protect fungal hyphae through chitin-

235 dependent polymerization of chitin-independent Mg1LysM homodimers (Sánchez-Vallet

236 *et al.*, 2020). To assess whether this trait is shared by Mgx1LysM, the amino acid sequence

237 of Mgx1LysM was aligned with Mg1LysM, displaying an overall sequence identity of 44%

(Fig. 6A). As expected, the predicted three-dimensional structure of Mgx1LysM shows a typical LysM fold with two antiparallel β-sheets adjacent to two α-helices (Fig. 6B) (Bateman and Bycroft, 2000; Bielnicki *et al.*, 2006; Liu *et al.*, 2012; Sánchez-Vallet *et al.*, 2013; Sánchez-Vallet *et al.*, 2020). More importantly, similar to Mg1LysM, Mgx1LysM carries a relatively long N-terminal sequence (Fig. 6B). For Mg1LysM it was recently shown that this N-terminal tail of a single monomer runs antiparallel with the tail of another Mg1LysM monomer, leading to the formation of ligand-independent homodimers (Sánchez-Vallet *et al.*, 2020). Structural modelling of Mgx1LysM suggests that this LysM effector is also able to dimerize via its N-terminal tail (Fig. 6B).

Besides ligand-independent dimerization, the crystal structure of Mg1LysM furthermore revealed chitin-dependent dimerization of the ligand-independent homodimers (Sánchez-Vallet *et al.*, 2020). Based on further biochemical evidence the occurrence of chitin-induced polymeric complexes was demonstrated (Sánchez-Vallet *et al.*, 2020). Thus, to assess whether Mgx1LysM similarly undergoes chitin-induced polymerization, a previously developed centrifugation assay was performed using *E. coli*-produced Mgx1LysM (Sánchez-Vallet *et al.*, 2020), with Ecp6 as negative control and Mg1LysM and RiSLM as positive controls. Like Mg1LysM also RiSLM, a LysM effector from the arbuscular mycorrhizal fungus *Rhizophagus irregularis*, has been shown to undergo chitin-induced polymerization (Sánchez-Vallet *et al.*, 2020). After incubation with chitin, protein samples were centrifuged at 20,000 g in the presence of 0.002% methylene blue to visualize the protein. Similar as for Mg1LysM and RiSLM, a clear Mgx1LysM pellet emerged upon incubation with chitin, and not in the absence of chitin, while no chitin-induced polymerisation was observed for Ecp6 (Fig. 6C). Collectively, our data indicate that Mgx1LysM, like Mg1LysM, undergoes not only chitin-dependent dimerization, but also ligand-independent dimerization through interactions at the N-termini of Mgx1LysM

263 monomers, leading to polymerization of the LysM effector protein in the presence of

264 chitin.

265

266 **DISCUSSION**

267 In this study, we demonstrate that the previously disregarded LysM effector gene as a

268 presumed pseudogene of the fungal wheat pathogen *Z. tritici*, *Mgx1LysM*, is a functional

269 LysM effector gene that plays a role in *Z. tritici* virulence during infection of wheat plants.

270 Like the previously characterized *Z. tritici* LysM effectors Mg1LysM and Mg3LysM,

271 Mgx1LysM binds chitin (Fig. 3), suppresses chitin-induced ROS production (Fig. 4) and

272 can protect fungal hyphae against chitinase hydrolysis (Fig. 5). Moreover, like Mg1LysM,

273 Mgx1LysM polymerizes in the presence of chitin (Fig. 6). Through these activities,

274 Mgx1LysM makes a noticeable contribution to *Z. tritici* virulence on wheat plants (Fig. 2).

275   Merely based on expression profile as well as biological activities, the three genes

276 seem to behave in a similar fashion and complete redundancy could be expected. However,

277 this is not what we observed in the mutant analyses, as these revealed that Mg3LysM

278 confers the largest contribution, as targeted deletion of *Mg3LysM*, but not of Mg1LysM or

279 Mgx1LysM, results in a noticeable difference in symptomatology. Moreover, even the

280 simultaneous deletion of *Mgx1LysM* and *Mg1LysM* did not lead to compromised necrosis

281 development, although deletion of these two genes from the *Mg3LysM* deletion strain in

282 the triple mutant resulted in a further decrease of virulence. Thus, although it can be

283 concluded that all three LysM effectors contribute to fungal virulence, these findings are

284 suggestive of partially redundant and partially additive activities. This suggestion is

285 further reinforced when assessing pycnidia development and fungal colonization data

286 that demonstrate that single LysM effector deletions have significant effects on these

287 traits. However, it presently remains unknown through which functional divergence these

288 differential phenotypes are established.

289   The ability to protect fungal hyphae against chitinase hydrolysis that is shared by

290 the three *Z. tritici* LysM effectors (Fig. 5) has previously been recorded for some, but not

291 all, LysM effectors from other fungal species as well. For example, although *Verticillium*

292 *dahliae* Vd2LysM and *Rhizophagus irregularis* RiSLM can protect hyphae as well

293 (Kombrink *et al.*, 2017; Zeng *et al.*, 2020), *C. fulvum* Ecp6, *Colletotrichum higginsianum*

294 ChElp1 and ChElp2, and *Magnaporthe oryzae* MoSlp1 do not possess such activity (de

295 Jonge *et al.*, 2010; Mentlak *et al.*, 2012; Takahara *et al.*, 2016). Intriguingly, all LysM

296 effectors that contain a single LysM characterized to date (Mg1LysM, Mgx1LysM, RiSLM)

297 were found to protect fungal hyphae. However, among the ones with two LysM domains

298 members are found that do (Vd2LysM) and that do not (ChElp1, ChElp2, MoSlp1) protect,

299 which is also true for members with three LysMs (Mg3LysM versus Ecp6, respectively),

300 suggesting that the ability to protect hyphae is not determined by the number of LysMs in

301 the effector protein. Previously, a mechanistic explanation for the ability to protect fungal

302 cell wall chitin has been provided for the *C. fulvum* effector protein Avr4 that acts as a

303 functional homolog of LysM effectors that protect fungal hyphae, but that binds chitin

304 through an invertebrate chitin-binding domain (CBM14) rather than through LysMs (van

305 den Burg *et al.*, 2006). Intriguingly, Avr4 strictly interacts with chitotriose, but binding of

306 additional Avr4 molecules to chitin occurs through cooperative interactions between

307 Avr4 monomers, which can explain the effective shielding of cell wall chitin (van den Burg

308 *et al.*, 2004). Despite being a close relative of *C. fulvum* in the Dothidiomycete class of

309 Ascomycete fungi, *Z. tritici* lacks an Avr4 homolog (Stergiopoulos *et al.*, 2010). This may

310 explain why the *Z. tritici* LysM effectors, in contrast to *C. fulvum* Ecp6, evolved the ability

311 to protect fungal cell wall chitin. Recently, it has been proposed that the hyphal protection

by LysM effectors that contain only a single LysM, including Mg1LysM and RiSLM, is due

to chitin-induced polymerisation, leading to contiguous LysM effector filaments that are

anchored to chitin in the fungal cell wall to protect these cell walls (Sánchez-Vallet *et al.*,

2020). Here, we show that Mgx1LysM similarly undergoes chitin-induced polymer

formation (Fig. 6).

It was previously reported that Mg1LysM was incapable of suppressing chitin-

induced immune responses (Marshall *et al.*, 2011), in contrast to the immune-suppressive

activity of Mg3LysM. A mechanistic explanation for this observation was found in the

observation that Ecp6, being a close homolog of Mg3LysM, was able to efficiently

sequester chitin oligomers from host receptors through intramolecular LysM

dimerization, leading to a binding groove with ultra-high chitin-binding affinity. As a

single LysM-containing effector protein, Mg1LysM lacks the ability to undergo

intramolecular LysM dimerization, and thus to form an ultra-high affinity groove for chitin

binding, which could explain the inability to suppress immune responses by out-

competition of host receptor molecules for chitin binding. However, this mechanistic

explanation was recently challenged by data showing that the *R. irregulars* RiSLM is able

to suppress chitin-triggered immunity as well (Zeng *et al.*, 2020). In the present study we

show that not only Mgx1LysM can suppress chitin-triggered immunity, but also that

Mg1LysM possesses this activity (Fig. 4). However, it needs to be acknowledged that

whereas we used *P. pastoris*-produced protein in our initial analyses (Marshall *et al.*,

2011), we used *E. coli*-produced protein in the current study. More recent insights after

the publication of our initial study have revealed that LysM effector proteins may bind

chitin fragments that are released from the *P. pastoris* cell walls during protein production,

which may compromise the activity of the protein preparation in subsequent assays

(Kombrink *et al.*, 2017; Sánchez-Vallet *et al.*, 2013; Sánchez-Vallet *et al.*, 2020). As the *E.*

337   *coli* cell wall is devoid of chitin, partially or fully inactive protein preparations due to

338   occupation of the substrate binding site are unlikely to occur. However, since Mg1LysM,

339   Mgx1LysM and RiSLM are able to suppress chitin-triggered immunity, a mechanistic

340   explanation needs to be provided for the suppressive activity that does not involve

341   substrate sequestration purely based on chitin-binding affinity. Possibly, these LysM

342   effectors are able to perturb the formation of active chitin receptor complexes by binding

343   to receptor monomers in a similar fashion as has been proposed for LysM2 of Ecp6

344   (Sánchez-Vallet *et al.*, 2013; Sánchez-Vallet *et al.*, 2015) to prevent the activation of chitin-

345   triggered immune responses. Alternatively, precipitation of polymeric complexes formed

346   by LysM effectors and released chitin oligosaccharides may provide a mechanism to

347   eliminate these oligosaccharides and prevent their interaction with host receptor

348   molecules.

349

MATERIALS AND METHODS

351   **Gene expression analysis**

352   Total RNA was isolated using the RNeasy Plant Mini Kit (Qiagen, Maryland, USA). For each

353   sample, 2 μg RNA was used for cDNA synthesis with M-MLV Reverse Transcriptase

354   (Promega, Madison, USA) and 1 μL of the obtained cDNA was used for real-time PCR with

355   SYBR™ green master mix (Bioline, Luckenwalde, Germany) on a C1000 Touch™ Thermal

356   Cycler (Bio-Rad, California, USA). Expression of *Mgx1LysM* was normalized to the *Z. tritici*

357   housekeeping gene *β-tubulin* using primer pairs *Mgx1LysM*-F/*Mgx1LysM*-R and *ZtβTUB*-

358   F1/R1, respectively (Table S1). Relative expression was calculated with the $E^{-\Delta Ct}$ method

359   and the boxplot was made with RStudio using the package of ggplot2 (R Core Team, 2017;

360   Wickham, 2016).

361

Heterologous protein production in *E. coli*

363 Signal peptide prediction was performed using SignalP 5.0

364 (http://www.cbs.dtu.dk/services/SignalP/). The coding region for the mature Mgx1LysM

365 protein was amplified from *Z. tritici* IPO323 genomic cDNA using primers *Mgx1LysM*-

366 cDNA-F/ R (Table S1) and cloned into the pETSUMO vector and transformed as

367 pETSUMO-Mgx1LysM into *E. coli* strain Origami for heterologous protein production as a

368 fusion protein with a 6×His-SUMO affinity-tag. *Mgx1LysM* expression was induced with

369 0.2 mM isopropyl β-D-1-thiogalactopyranoside (IPTG) at 28°C overnight. Next, *E. coli* cells

370 were harvested by centrifugation at 3,800 g for one hour and resuspended in 20 mL cell

371 lysis buffer (50 mM Tris-HCl pH 8.5, 150 mM NaCl, 2 mL glycerol, 120 mg lysozyme, 40

372 mg deoxycholic acid, 1.25 mg DNase I and 1 protease inhibitor pill) and incubated at 4°C

373 for two hours with stirring, and centrifuged at 20,000 g for one hour. The resulting cleared

374 supernatant was immediately placed on ice and subjected to further purification.

375 The His60 Ni Superflow Resin (Clontech, California, USA) was used for Mgx1LysM

376 purification and first equilibrated with wash buffer (50 mM Na_2HPO_4, 150 mM NaCl, 10

377 mM imidazole, pH 8.0) after which the protein preparation was loaded on the column. The

378 target protein was eluted with elution buffer (50 mM Na_2HPO_4, 150 mM NaCl, 300 mM

379 imidazole, pH 8.0), and purity of the elution was tested on an SDS-PAGE gel followed by

380 Coomassie brilliant blue (CBB) staining. The 6×His-SUMO affinity-tag was cleaved with

381 the SUMO Protease ULP1 during overnight dialysis against 200 mM NaCl. Non-cleaved

382 Mgx1LysM fusion protein was removed using His60 Ni Superflow resin, and the flow-

383 through with cleaved Mgx1LysM was adjusted to the required concentration.

384

385 **Chitin binding assay**

386 *E. coli*-produced proteins were adjusted to a concentration of 30 μg/mL in chitin binding

387 buffer (50 mM Tris PH 8.0, 150 mM NaCl) and 800 μL of protein solution was incubated

388 with 50 μL of magnetic chitin beads, or 5 mg of crab shell chitin, cellulose or xylan in a

389 rotary shaker at 4°C for 6h. The insoluble fraction was pelleted by centrifuging at 13,500

390 g for 5 min and resuspend in 100 μL demineralized water. Supernatants were collected

391 into Microcon Ultracel YM-10 tubes (Merck, Darmstadt, Germany) and concentrated a

392 volume of approximately 100 μL. For each of the insoluble carbohydrates, 30 μL of the

393 pellet solution and the concentrated supernatant was incubated with 10 μL of SDS-PAGE

394 protein loading buffer (4×; 200 mM Tris-HCl, pH 6.5, 0.4 M dithiothreitol, 8 % sodium

395 dodecyl sulfate, 6 mM bromophenol blue, 40 % glycerol) and incubated at 95°C for 10

396 min. Samples were loaded into an SDS-PAGE gel followed by CBB staining.

397

398 **Hyphal protection against chitinase hydrolysis**

399 *Trichoderma viride* conidiospores were harvested from five-day-old potato dextrose agar

400 (PDA; OXOID, Basingstoke, United Kingdom), washed with sterile water, and adjusted to

401 a concentration of 10^6 spores/mL with potato dextrose broth (PDB; Becton Dickinson,

402 Maryland, USA). Conidiospore suspensions were dispensed into a 96-well microtiter plate

403 in aliquots of 50 μL and incubated at room temperature overnight. Effector proteins were

404 added to a final concentration of 10 μM, and after 2 h of incubation 3 μL of chitinase from

405 *Clostridium thermocellum* (Creative Enzymes, New York, USA) or 10 μL of crude extract of

406 tomato chitinases was added into the appropriate wells. As control, sterile water was

407 added. All treatments were further incubated for 4 h and hyphal growth was inspected

408 with a Nikon H600L microscope.

409

Reactive oxygen species measurement

411 Reactive oxygen species (ROS) production measurements were performed using three

412 *Nicotiana benthamiana* leaf discs (Ø = 0.5 cm) per treatment, which were collected from

413 two-week-old *N. benthamiana* plants, placed into a 96-well microtiter plate, and rinsed

414 with 200 µL demineralized water. After 24 hours the water was replaced by 50 µL fresh

415 demineralized water and the plate was incubated for another hours at room temperature.

416 Meanwhile, mixtures of $(GlcNAc)_6$ (IsoSep AB, Tullinge, Sweden) and effector proteins

417 were incubated for two hours. In total, 20 µL of $(GlcNAc)_6$ was added in a final

418 concentration of 10 µM to trigger ROS production in the absence or presence of 100 µL of

419 effector protein in a final concentration of 50 µM in measuring solution containing 100

420 µM L-012 substrate (FUJIFILM, Neuss, Germany) and 40 µg/mL horseradish peroxidase

421 (Sigma-Aldrich, Missouri, USA). Chemiluminescence measurements were taken every

422 minute over 30 min in a CLARIOstar microplate reader (BMG LABTECH, Ortenberg,

423 Germany).

424

***Agrobacterium tumefaciens*-mediated *Z. tritici* transformation**

426 To generate *Mgx1LysM* deletion mutants, approximately 1.0 kb upstream and 1.2 kb

427 downstream fragments of *Mgx1LysM* were amplified from genomic DNA of *Z. tritici*

428 IPO323 using primer pairs *Mgx1LysM*-userL-F/R and *Mgx1LysM*-userR-F/R (Table S1)

429 and the amplicons were cloned into vector pRF-NU2 as previously described (Frandsen

430 et al, 2008). The resulting deletion construct was transformed into *Z. tritici* mutant *Δku70*

431 and the previously generated *ΔMg1LysM*, *ΔMg3LysM* and *ΔMg1-ΔMg3* to generate double-

432 and triple-gene deletion mutants. In short, minimal medium (MM) and induction medium

433 (IM) were prepared at a pH of 7.0 and *Z. tritici* conidiospores were collected, washed and

434 adjusted to a final concentration of 10^7 spores/mL. Transformation plates were incubated

435   at 16°C in dark for two to three weeks. Putative transformants were transferred to PDA

436   plates supplemented with 200 µg/mL cefotaxime and 25 µg/mL nourseothricin (Sigma-

437   Aldrich, Missouri, USA) and absence of *Mgx1LysM* was confirmed with PCR using the gene-

438   specific primers *Mgx1LysM*-F/*Mgx1LysM*-R and the primers *NAT*-F/R (Table S1).

439

440   **Gene copy number determination**

441   The copy number of the *NAT* resistance marker gene was determined with real-time PCR

442   using primers *NAT*-F/R and *ZtβTUB*-F2/R2 (Table S1). The primer efficiency was

443   determined using a series of 10x dilutions of the genomic DNAs extracted from the triple-

444   gene deletion strain *ΔMg1-ΔMgx1-ΔMg3* (392 ng/µL) and the wild-type strain IPO323

445   (600 ng/µL). Real-time PCR assays were performed with an annealing temperature of

446   66°C at which the calculated efficiencies of both primer pairs approached 100%. The Ct

447   value of *NAT* was normalized to the single-copy gene *β-tubulin* and calculated with the E-

448      $^{\Delta Ct}$ method.

449

450   ***Z. tritici* inoculations on wheat**

451   For all inoculation assays, the wheat cultivar "Riband" was used. *Z. tritici* wild-type strain

452   IPO323 and the mutants were grown either on yeast extract peptone dextrose (YPD; 10 g

453   yeast extract/L, 20 g peptone/L, 20 g dextrose and 15 g agar/L) or in yeast glucose

454   medium (YGM; 10 g yeast extract/L, 30 g glucose/L) supplemented with appropriate

455   antibiotics at 16°C with orbital shaking (100 rpm) for at least five days to obtain yeast-

456   like conidiospores that were used for plant inoculation. To this end, conidiospores were

457   collected by centrifuging the suspensions at 2,000 g for 5 min and adjustment to a final

458   concentration of 10^7 spores/mL with 0.5% Tween 20 for inoculation by brushing on

459   adaxial and abaxial sides of primary leaves of 11-day-old wheat plants. The inoculated

460 plants were covered in a plastic tent for two days to secure high humidity, after which the

461 tent was opened in one-side.

462 Fungal biomass was measured with real-time PCR using a C1000 Touch™ Thermal

463 Cycler (Bio-Rad, California, USA) with the *Z. tritici*-specific *β-tubulin* primers *ZtβTUB*-

464 F1/R1 in combination with primers *TaCDC*-F/R that target the constitutively expressed

465 cell division control gene of wheat (Table S1). Relative fungal biomass was calculated with

466 the $E^{-\Delta Ct}$ method and boxplots were made with RStudio using the package of ggplot2 (R

467 Core Team, 2017; Wickham, 2016).

468

Protein structure prediction and polymerization assay

469

470 Three-dimensional structures of Mgx1LysM was predicted with I-TASSER server (Roy *et*

471 *al.*, 2010; Yang and Zhang, 2015). For chitin-induced polymerization assay of LysM

472 effectors, concentrations of Mgx1LysM, Mg1LysM, RiSLM and Ecp6 were adjusted to 200

473 µM and 200 µL of each protein was incubated with 200 µL of 2 mM chitohexaose

474 (Megazyme, Wicklow, Ireland), or 200 µL water as control, at room temperature

475 overnight. The next day, 2 µL of 0.2% methylene blue (Sigma-Aldrich, Missouri, USA) was

476 added and incubated for 30 min after which protein solutions were centrifuged at 20,000

477 g for 15 min. Photos were taken with a ChemiDoc MP system (Bio-Rad, California, USA)

478 with custom setting for RFP.

479

489

490 **DATA AVAILABILITY STATEMENT**

491 Data available on request from the authors.

492

493 **AUTHORSHIP CONTRIBUTIONS**

494 HT, LRM, JRM, BPHJT conceived the study; HT, CIM and LRM designed experiments; HT,

495 CIM and GCMB performed experiments; HT analyzed data and wrote the manuscript; JJR

496 and HC provided experimental materials, JRM and BPHJT supervised the project; all

497 authors discussed the results and contributed to the final manuscript.

498

499 **CONFLICT OF INTEREST**

500 The authors declare no conflict of interest exists.

REFERENCES

Altenbach, D. and Robatzek, S. (2007) Pattern recognition receptors: from the cell surface to intracellular dynamics. *Mol. Plant-Microbe Interact.* **20**, 1031–1039.

Bateman, A. and Bycroft, M. (2000) The structure of a LysM domain from *E. coli* membrane-bound lytic murein transglycosylase D (MltD). *J. Mol. Biol.* **299**, 1113–1119.

Bielnicki, J., Devedjiev, Y., Derewenda, U., Dauter, Z., Joachimiak, A. and Derewenda, Z.S. (2006) *B. subtilis* ykuD protein at 2.0 A resolution: insights into the structure and function of a novel, ubiquitous family of bacterial enzymes. *Proteins* **62**, 144–151.

Boller, T. and Felix, G. (2009) A renaissance of elicitors: perception of microbe-associated molecular patterns and danger signals by pattern-recognition receptors. *Annu. Rev. Plant Biol.* **60**, 379–406.

Bolton, M.D., Esse, H.P. Van, Vossen, J.H., et al. (2008) The novel *Cladosporium fulvum* lysin motif effector Ecp6 is a virulence factor with orthologues in other fungal species. *Mol. Microbiol.* **69**, 119–136.

Bowler, J., Scott, E., Tailor, R., Scalliet, G., Ray, J. and Csukai, M. (2010) New capabilities for *Mycosphaerella graminicola* research. *Mol. Plant Pathol.* **11**, 691–704.

Burg, H.A. van den, Harrison, S.J., Joosten, M.H., Vervoort, J. and Wit, P.J. de (2006) *Cladosporium fulvum* Avr4 protects fungal cell walls against hydrolysis by plant chitinases accumulating during infection. *Mol. Plant-Microbe Interact.* **19**, 1420–1430.

Burg, H.A. van den, Spronk, C.A., Boeren, S., Kennedy, M.A., Vissers, J.P., Vuister, G.W., Wit, P.J. de and Vervoort, J. (2004) Binding of the AVR4 elicitor of *Cladosporium*

523 *fulvum* to chitotriose units is facilitated by positive allosteric protein-protein

524 interactions: the chitin-binding site of AVR4 represents a novel binding site on the

525 folding scaffold shared between the inverte. *J. Biol. Chem.* **279**, 16786–16796.

526 **Cao, Y., Liang, Y., Tanaka, K., Nguyen, C.T., Jedrzejczak, R.P., Joachimiak, A. and**

527 **Stacey, G.** (2014) The kinase LYK5 is a major chitin receptor in Arabidopsis and

528 forms a chitin-induced complex with related kinase CERK1. *Elife* **3**, 1–19.

529 **Cook, D.E., Mesarich, C.H. and Thomma, B.P.** (2015) Understanding plant immunity as

530 a surveillance system to detect invasion. *Annu. Rev. Phytopathol.* **53**, 541–563.

531 **Dolfors, F., Holmquist, L., Dixelius, C. and Tzelepis, G.** (2019) A LysM effector protein

532 from the basidiomycete *Rhizoctonia solani* contributes to virulence through

533 suppression of chitin-triggered immunity. *Mol. Genet. Genomics* **294**, 1211–1218.

534 **Dubey, M., Vélëz, H., Broberg, M., Jensen, D.F. and Karlsson, M.** (2020) LysM proteins

535 regulate fungal development and contribute to hyphal protection and biocontrol

536 traits in *Clonostachys rosea*. *Front. Microbiol.* **11**, 1–19.

537 **Esse, H.P. van, Bolton, M.D., Stergiopoulos, I., Wit, P.J.G.M. de and Thomma, B.P.H.J.**

538 (2007) The chitin-binding *Cladosporium fulvum* effector protein Avr4 is a virulence

539 factor. *Mol. Plant-Microbe Interact.* **20**, 1092–1101.

540 **Eyal, Z.** (1999) The Septoria tritici and Stagonospora nodorum blotch diseases of wheat.

541 *Eur. J. Plant Pathol.* **105**, 13.

542 **Felix, G., Regenass, M. and Boller, T.** (1993) Specific perception of subnanomolar

543 concentrations of chitin fragments by tomato cells: Induction of extracellular

544 alkalinization, changes in protein phosphorylation, and establishment of a refractory

545   state. *Plant J.* **4**, 307–316.

546   **Free, S.J.** (2013) Fungal cell wall organization and biosynthesis. *Adv. Genet.* **81**, 33–82.

547   **Fujikawa, T., Kuga, Y., Yano, S., Yoshimi, A., Tachiki, T., Abe, K. and Nishimura, M.**

548   (2009) Dynamics of cell wall components of *Magnaporthe grisea* during infectious

549   structure development. *Mol. Microbiol.* **73**, 553–570.

550   **Fujikawa, T., Sakaguchi, A., Nishizawa, Y., Kouzai, Y., Minami, E., Yano, S., Koga, H.,**

551   **Meshi, T. and Nishimura, M.** (2012) Surface alpha-1,3-glucan facilitates fungal

552   stealth infection by interfering with innate immunity in plants. *PLoS Pathog.* **8**,

553   e1002882.

554   **Gao, F., Zhang, B.-S., Zhao, J.-H., Huang, J.-F., Jia, P.-S., Wang, S., Zhang, J., Zhou, J.-M.**

555   **and Guo, H.-S.** (2019) Deacetylation of chitin oligomers increases virulence in soil-

556   borne fungal pathogens. *Nat. Plants* **5**, 1167–1176.

557   **Glazebrook, J.** (2005) Contrasting mechanisms of defense against biotrophic and

558   necrotrophic pathogens. *Annu. Rev. Phytopathol.* **43**, 205–227.

559   **Gueddari, N.E. El, Rauchhaus, U., Moerschbacher, B.M. and Deising, H.B.** (2002)

560   Developmentally regulated conversion of surface-exposed chitin to chitosan in cell

561   walls of plant pathogenic fungi. *New Phytol.* **156**, 103–112.

562   **Jashni, M.K., Dols, I.H., Iida, Y., Boeren, S., Beenen, H.G., Mehrabi, R., Collemare, J. and**

563   **Wit, P.J. de** (2015) Synergistic action of a metalloprotease and a serine protease from

564   *Fusarium oxysporum* f. sp. lycopersici cleaves chitin-binding tomato chitinases,

565   reduces their antifungal activity, and enhances fungal virulence. *Mol. Plant-Microbe*

566   *Interact.* **28**, 996–1008.

567 **Jones, J.D.G. and Dangl, J.L.** (2006) The plant immune system. *Nature* **444**, 323–329.

568 **Jonge, R. de, Esse, P. van, Kombrink, A., et al.** (2010) Conserved fungal LysM effector

569 Ecp6 prevents chitin-triggered immunity in plants. *Science (80-.).* **329**, 953–955.

570 **Jonge, R. de and Thomma, B.P.H.J.** (2009) Fungal LysM effectors: extinguishers of host

571 immunity? *Trends Microbiol.* **17**, 151–157.

572 **Karisto, P., Hund, A., Yu, K., Anderegg, J., Walter, A., Mascher, F., McDonald, B.A. and**

573 **Mikaberidze, A.** (2018) Ranking quantitative resistance to septoria tritici blotch in

574 elite wheat cultivars using automated image analysis. *Phytopathology* **108**, 568–581.

575 **Kema, G.H.J., Yu, D.Z., Rijkenberg, F.H.J., Shaw, M.W. and Baayen, R.P.** (1996)

576 Histology of the pathogenesis of *Mycosphaerella graminicola* in wheat.

577 *Phytopathology* **86**, 777–786.

578 **Kombrink, A., Rovenich, H., Shi-Kunne, X., et al.** (2017) *Verticillium dahliae* LysM

579 effectors differentially contribute to virulence on plant hosts. *Mol. Plant Pathol.* **18**,

580 596–608.

581 **Kombrink, A., Sánchez-Vallet, A. and Thomma, B.P.H.J.** (2011) The role of chitin

582 detection in plant-pathogen interactions. *Microbes Infect.* **13**, 1168–1176.

583 **Kombrink, A. and Thomma, B.P.H.J.** (2013) LysM effectors: secreted proteins

584 supporting fungal life. *PLOS Pathog.* **9**, e1003769.

585 **Lee, W.S., Rudd, J.J., Hammond-Kosack, K.E. and Kanyuka, K.** (2014) *Mycosphaerella*

586 *graminicola* LysM effector-mediated stealth pathogenesis subverts recognition

587 through both CERK1 and CEBiP homologues in wheat. *Mol. Plant-Microbe Interact.*

588 **27**, 236–243.

589 **Liu, T., Liu, Z., Song, C., et al.** (2012) Chitin-induced dimerization activates a plant

590 immune receptor. *Science (80-.).* **336**, 1160–1164.

591 **Marshall, R., Kombrink, A., Motteram, J., Loza-Reyes, E., Lucas, J., Hammond-Kosack,**

592 **K.E., Thomma, B.P.H.J. and Rudd, J.J.** (2011) Analysis of two in planta expressed

593 LysM effector homologs from the fungus *Mycosphaerella graminicola* reveals novel

594 functional properties and varying contributions to virulence on wheat. *Plant Physiol.*

595 **156**, 756–769.

596 **Mauch, F., Mauch-Mani, B. and Boller, T.** (1988) Antifungal hydrolases in pea tissue: II.

597 Inhibition of fungal growth by combinations of chitinase and β-1,3-glucanase. *Plant*

598 *Physiol.* **88**, 936–942.

599 **Mentlak, T.A., Kombrink, A., Shinya, T., et al.** (2012) Effector-mediated suppression of

600 chitin-triggered immunity by *Magnaporthe oryzae* is necessary for rice blast disease.

601 *Plant Cell* **24**, 322–335.

602 **Miya, A., Albert, P., Shinya, T., et al.** (2007) CERK1, a LysM receptor kinase, is essential

603 for chitin elicitor signaling in Arabidopsis. *Proc Natl Acad Sci U S A* **104**, 19613–19618.

604 **Pnini-Cohen, S., Zilberstein, A., Schuster, S., Sharon, A. and Eyal, Z.** (2000) Elucidation

605 of Septoria tritici x wheat interactions using GUS-expressing isolates. *Phytopathology*

606 **90**, 297–304.

607 **Ride, J.P. and Barber, M.S.** (1990) Purification and characterization of multiple forms of

608 endochitinase from wheat leaves. *Plant Sci.* **71**, 185–197.

609 **Rovenich, H., Boshoven, J.C. and Thomma, B.P.H.J.** (2014) Filamentous pathogen

610 effector functions: Of pathogens, hosts and microbiomes. *Curr. Opin. Plant Biol.* **20**,

611   96–103.

612   **Roy, A., Kucukural, A. and Zhang, Y.** (2010) I-TASSER: a unified platform for automated

613   protein structure and function prediction. *Nat Protoc* **5**, 725–738.

614   **Rudd, J.J., Kanyuka, K., Hassani-Pak, K., et al.** (2015) Transcriptome and metabolite

615   profiling of the infection cycle of *Zymoseptoria tritici* on wheat reveals a biphasic

616   interaction with plant immunity involving differential pathogen chromosomal

617   contributions and a variation on the hemibiotrophic lifestyle def. *Plant Physiol.* **167**,

618   1158–1185.

619   **Rudd, J.J., Keon, J. and Hammond-Kosack, K.E.** (2008) The wheat mitogen-activated

620   protein kinases TaMPK3 and TaMPK6 are differentially regulated at multiple levels

621   during compatible disease interactions with *Mycosphaerella graminicola*. *Plant*

622   *Physiol.* **147**, 802–815.

623   **Sanchez-Vallet, A., Mesters, J.R. and Thomma, B.P.H.J.** (2015) The battle for chitin

624   recognition in plant-microbe interactions. *FEMS Microbiol. Rev.* **39**, 171–183.

625   **Sanchez-Vallet, A., Saleem-Batcha, R., Kombrink, A., Hansen, G., Valkenburg, D.J.,**

626   **Thomma, B.P.H.J. and Mesters, J.R.** (2013) Fungal effector Ecp6 outcompetes host

627   immune receptor for chitin binding through intrachain LysM dimerization. *Elife* **2**,

628   e00790.

629   **Sánchez-Vallet, A., Tian, H., Rodriguez-Moreno, L., et al.** (2020) A secreted LysM

630   effector protects fungal hyphae through chitin-dependent homodimer

631   polymerization. *PLoS Pathog.* **16**, 1–21.

632   **Shimizu, T., Nakano, T., Takamizawa, D., et al.** (2010) Two LysM receptor molecules,

633   CEBiP and OsCERK1, cooperatively regulate chitin elicitor signaling in rice. *Plant J.*

634   **64**, 204–214.

635   **Stergiopoulos, I., Burg, H.A. van den, Okmen, B., Beenen, H.G., Liere, S. van, Kema,**

636   **G.H. and Wit, P.J. de** (2010) Tomato Cf resistance proteins mediate recognition of

637   cognate homologous effectors from fungi pathogenic on dicots and monocots. *Proc*

638   *Natl Acad Sci U S A* **107**, 7610–7615.

639   **Takahara, H., Hacquard, S., Kombrink, A., et al.** (2016) *Colletotrichum higginsianum*

640   extracellular LysM proteins play dual roles in appressorial function and suppression

641   of chitin-triggered plant immunity. *New Phytol.* **211**, 1323–1337.

642   **Team, R.C.** (2017) R: A language and environment for statistical computing. *R Found. Stat.*

643   *Comput.*

644   **Thomma, B.P.H.J., Penninckx, I.A.M.A., Broekaert, W.F. and Cammue, B.P.A.** (2001)

645   The complexity of disease signaling in Arabidopsis. *Curr. Opin. Immunol.* **13**, 63–68.

646   **Wan, J., Tanaka, K., Zhang, X.-C., Son, G.H., Brechenmacher, L., Nguyen, T.H.N. and**

647   **Stacey, G.** (2012) LYK4, a lysin motif receptor-like kinase, is important for chitin

648   signaling and plant innate immunity in Arabidopsis. *Plant Physiol.* **160**, 396–406.

649   **Wickham, H.** (2016) ggplot2: Elegant Graphics for Data Analysis, Springer-Verlag New

650   York.

651   **Yang, J. and Zhang, Y.** (2015) I-TASSER server: new development for protein structure

652   and function predictions. *Nucleic Acids Res.* **43**, W174-81.

653   **Zeng, T., Rodriguez-Moreno, L., Mansurkhodzaev, A., et al.** (2020) A lysin motif

654   effector subverts chitin-triggered immunity to facilitate arbuscular mycorrhizal

655   symbiosis. *New Phytol.* **225**, 448–460.

656

FIGURE LEGENDS

Fig. 1 Expression of *Mgx1LysM* is induced in *Zymoseptoria tritici* upon inoculation on wheat plants. Relative expression of *Mgx1LysM* at 4, 8, 10 and 14 days post inoculation on wheat plants and upon growth *in vitro* in Czapek-dox (CDB) or potato dextrose broth (PDB) when normalized to *Z. tritici β-tublin*. The boxplot was made with RStudio using the package ggplot2.

Fig. 2 Mgx1LysM contributes to *Z. tritici* virulence on wheat and displays functional redundancy with Mg1LysM and Mg3LysM. (A) Disease symptoms on wheat leaves at 21 days post inoculation (dpi) with the wild-type strain (WT) and LysM effector gene deletion strains. (B) Quantification of the necrotic area on wheat leaves inoculated with WT and LysM effector gene deletion strains at 21 dpi. (C) Fungal biomass determined with real-time PCR on *Z. tritici β-tubulin* relative to the wheat cell division control gene, on wheat leaf samples harvested at 21 dpi. Graphs were made with RStudio using the package of ggplot2 and different letters indicating significant differences between each inoculation were calculated with IBM Statistics 26 with One-way ANOVA (Duncan; $P<0.05$). Fungal inoculation experiments were conducted on six plants with six first-primary leaves per inoculation and repeated twice with similar results.

Fig. 3 Mgx1LysM binds chitin. *E. coli*-produced Mgx1LysM and Mg1LysM were incubated with four chitin products for 6 hours and, after centrifugation, pellets and supernatants were analysed using polyacrylamide gel electrophoresis followed by CBB staining.

Fig. 4 Mgx1LysM suppresses the chitin-induced reactive oxygen species (ROS) burst. Leaf discs of *Nicotiana benthamiana* were treated with chitohexaose (chitin) to induce ROS production. Chitin was pre-incubated with Ecp6, Mg1LysM or Mgx1LysM for two hours and subsequently added to the leaf discs. Error bars represent standard errors from five biological replicates.

Fig. 5 Mgx1LysM protects hyphal growth of *Trichoderma viride* against chitinase hydrolysis. Microscopic pictures of *T. viride* grown *in vitro* with or without two hours of preincubation with *C. fulvum* Avr4, or *Z. tritici* Mg1LysM or Mgx1LysM, followed by the addition of chitinase or water. Pictures were taken ~4 hours after the addition of chitinase.

Fig. 6 Mgx1LysM undergoes chitin-induced polymerization. (A) Amino acid sequence alignment of Mgx1LysM and Mg1LysM. The LysM is indicated with black underlining. (B) I-TASSER software-based *in-silico* prediction of the three-dimensional structure of Mgx1LysM (left) based on the recently generated crystal structure of Mg1LysM (right) (Sánchez-Vallet et al., 2020). The *N*-terminal 15 amino acids of both proteins are depicted in orange. Structures are visualized using the PyMOL molecular graphics system (Schrodinger LLC, 2015). (C) The LysM effector Mgx1LysM, together with RiSLM and Mg1LysM as positive controls, and Ecp6 as negative control, were incubated with chitohexaose (chitin) or water. After overnight incubation, methylene blue was added and protein solutions were centrifuged, resulting in protein pellets (red arrowheads) as a consequence of polymerization for Mgx1LysM, Mg1LysM and RiSLM, but not for Ecp6.

703 **LEGENDS SUPPORTING INFORMATION**

704 **Fig. S1 Genotypic confirmation of the *Mgx1LysM* deletion strains of *Z. tritici*.** (A)

705 Agarose gel electrophoresis of the PCR products amplified from genomic DNA of the *Z.*

706 *tritici* wild-type (WT) and mutant strains. Primers Mgx-F/R and NAT-F/R were used to

707 confirm the absence of *Mgx1LysM* and presence of the *NAT* resistance marker gene. (B)

708 The *NAT* copy number in the genome of WT and mutant strains was determined by

709 normalizing to the single-copy *β-tubulin* (*ZtTUB*) gene with real-time PCR. The copy

710 number was calculated with the $E^{-\Delta Ct}$ method. The bar graph is made with RStudio with

711 the package ggplot2.

712

713 **Fig. S2 Pycnidia formation determined on wheat leaf samples inoculated with the**

714 **wild-type *Z. tritici* strain (WT) and gene deletion mutants.** harvested at 17 post

715 inoculation (dpi). Boxplot graph was made with RStudio using the package of ggplot2 and

716 different letters indicating significant differences between each inoculation were

717 calculated with IBM Statistics 26 with One-way ANOVA (Duncan; P<0.05).

718

719 **Fig. S3 Mgx1LysM protects hyphal growth of *Trichoderma viride* against the**

720 **hydrolysis by a crude extract of tomato leaves containing chitinases.** Microscopic

721 pictures of *T. viride* grown with or without preincubation with Mgx1LysM, followed by the

722 addition of a crude extract of tomato leaves containing chitinases. Pictures were taken 4

723 hours after chitinase addition.

1
2
3
4
5
6
7
8
9
10
11
12
13
14
15
16
17
18
19
20
21
22
23
24
25
26
27
28
29
30
31
32
33
34
35
36
37
38
39
40
41
42
43
44
45
46
47
48
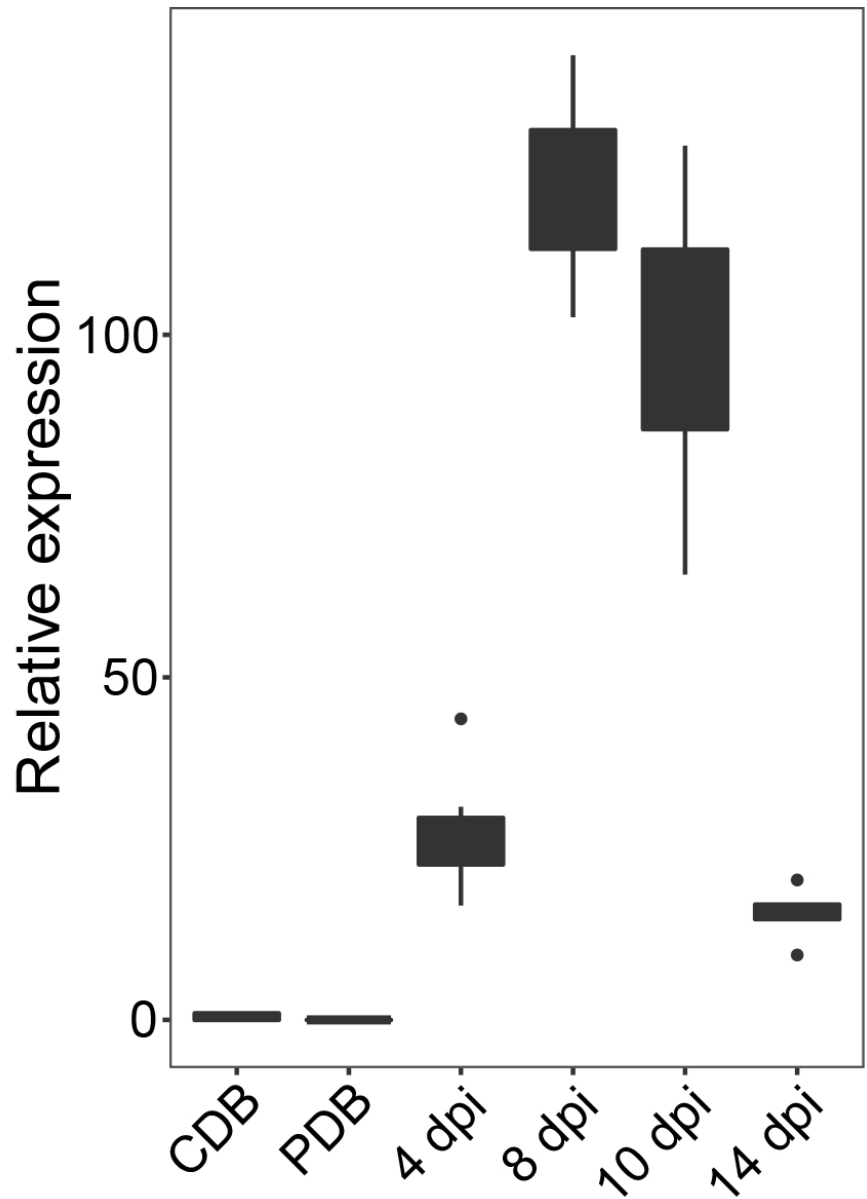49
50
51
52
53
54
55
56
57
58
59
60

Fig. 1 Expression of Mgx1LysM is induced in Zymoseptoria tritici upon inoculation on wheat plants. Relative expression of Mgx1LysM at 4, 8, 10 and 14 days post inoculation on wheat plants and upon growth in vitro in Czapek-dox (CDB) or potato dextrose broth (PDB) when normalized to Z. tritici β-tublin. The boxplot was made with RStudio using the package ggplot2.

Fig. 2 Mgx1LysM contributes to Z. tritici virulence on wheat and displays functional redundancy with Mg1LysM and Mg3LysM. (A) Disease symptoms on wheat leaves at 21 days post inoculation (dpi) with the wild-type strain (WT) and LysM effector gene deletion strains. (B) Quantification of the necrotic area on wheat leaves inoculated with WT and LysM effector gene deletion strains at 21 dpi. (C) Fungal biomass determined with real-time PCR on Z. tritici β-tubulin relative to the wheat cell division control gene, on wheat leaf samples harvested at 21 dpi. Graphs were made with RStudio using the package of ggplot2 and different letters indicating significant differences between each inoculation were calculated with IBM Statistics 26 with One-way ANOVA (Duncan; P<0.05). Fungal inoculation experiments were conducted on six plants with six first-primary leaves per inoculation and repeated twice with similar results.

1
2
3
4
5
6
7
8
9
10
11
12
13
14
15
16
17
18
19
20
21
22
23
24
25
26
27
28
29
30
31
32
33
34
35
36
37
38
39
40
41
42
43
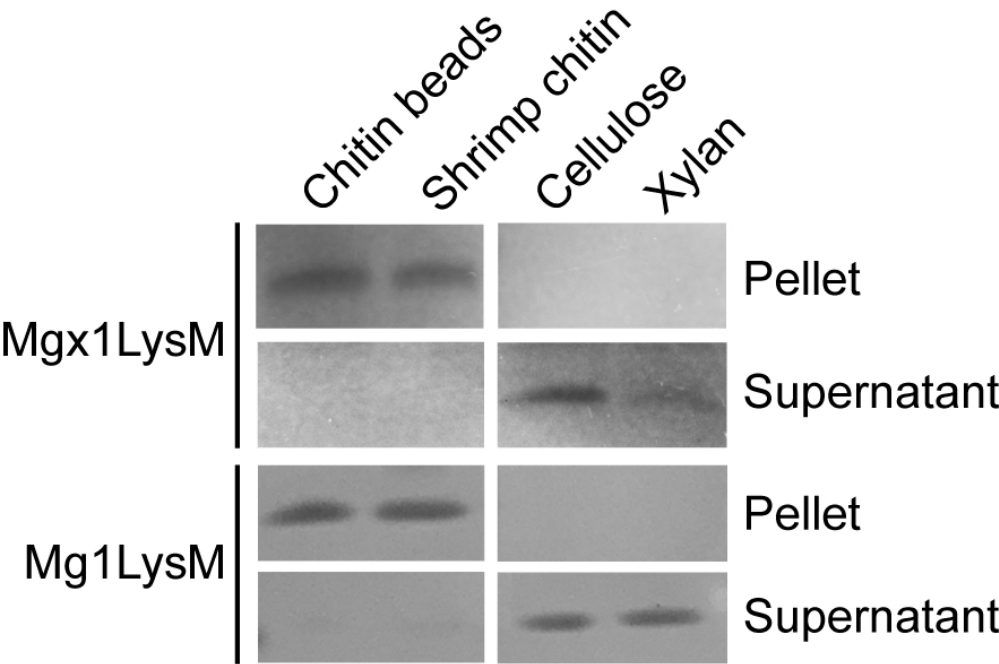44
45
46
47
48
49
50
51
52
53
54
55
56
57
58
59
60

Fig. 3 Mgx1LysM binds chitin. E. coli-produced Mgx1LysM and Mg1LysM were incubated with four chitin products for 6 hours and, after centrifugation, pellets and supernatants were analysed using polyacrylamide gel electrophoresis followed by CBB staining.
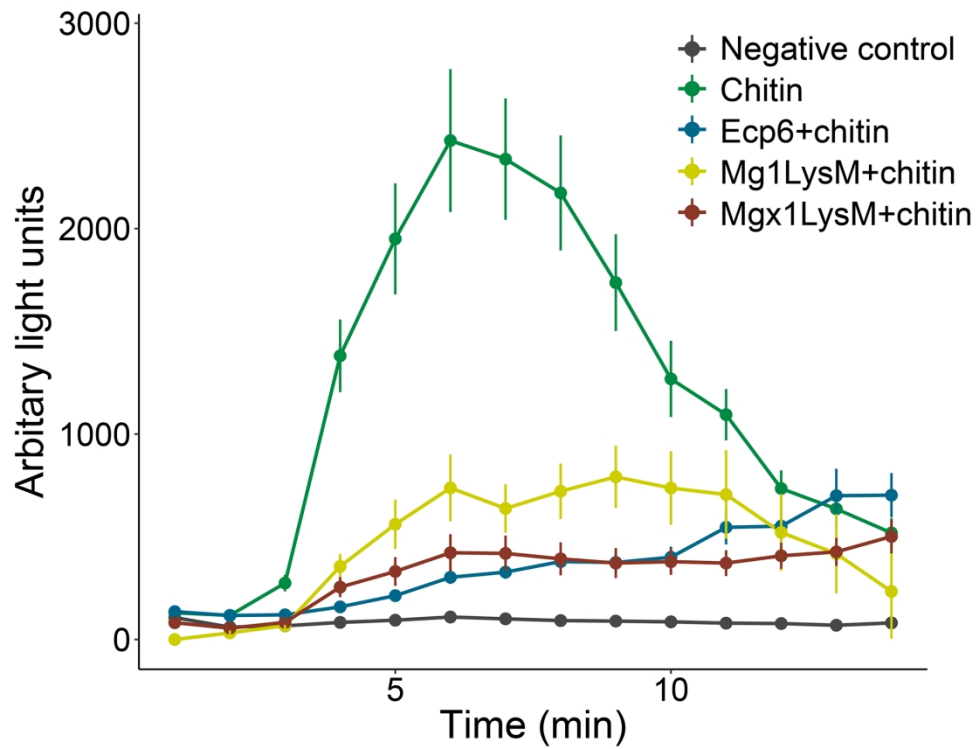
Fig. 4 Mgx1LysM suppresses the chitin-induced reactive oxygen species (ROS) burst. Leaf discs of Nicotiana benthamiana were treated with chitohexaose (chitin) to induce ROS production. Chitin was pre-incubated with Ecp6, Mg1LysM or Mgx1LysM for two hours and subsequently added to the leaf discs. Error bars represent standard errors from five biological replicates.
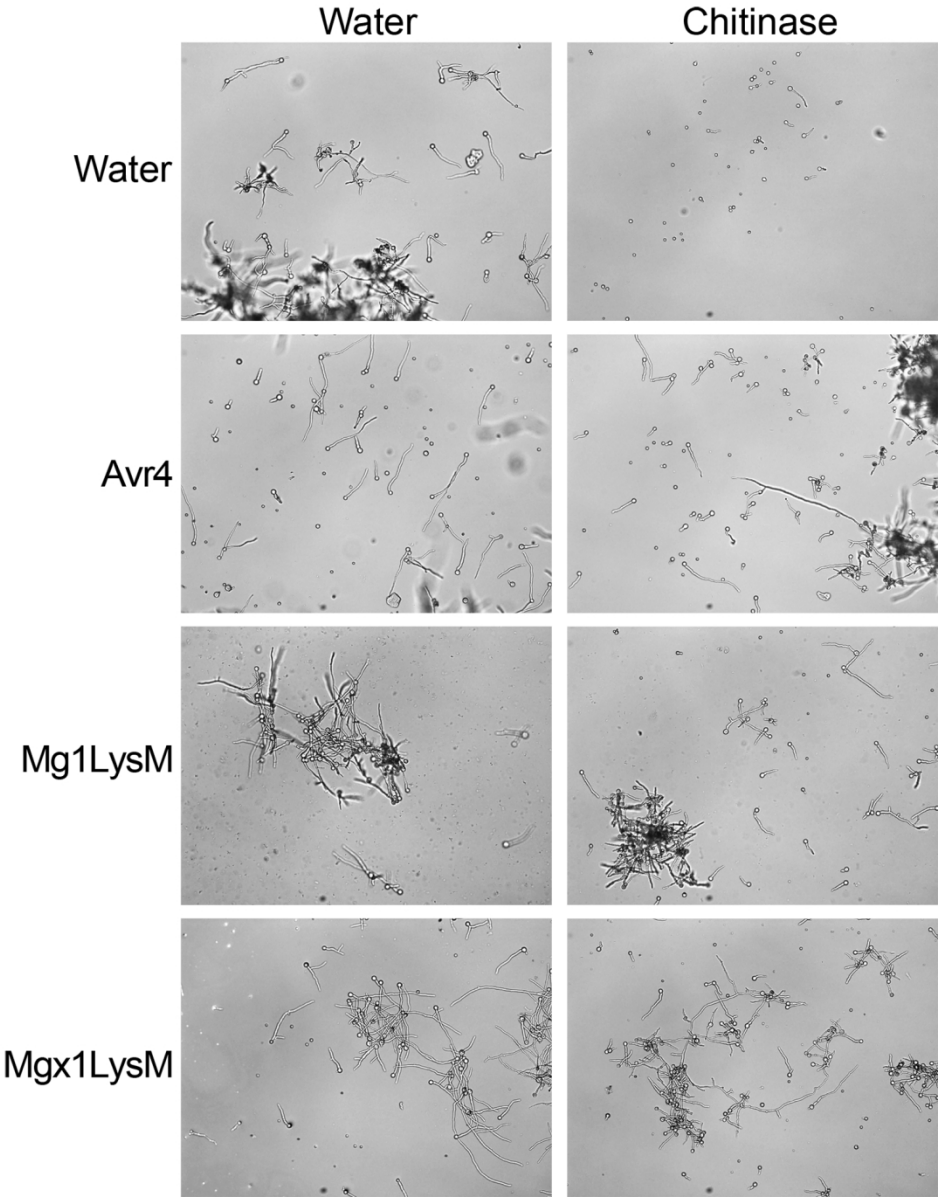
Fig. 5 Mgx1LysM protects hyphal growth of Trichoderma viride against chitinase hydrolysis. Microscopic pictures of T. viride grown in vitro with or without two hours of preincubation with C. fulvum Avr4, or Z. tritici Mg1LysM or Mgx1LysM, followed by the addition of chitinase or water. Pictures were taken ~4 hours after the addition of chitinase.
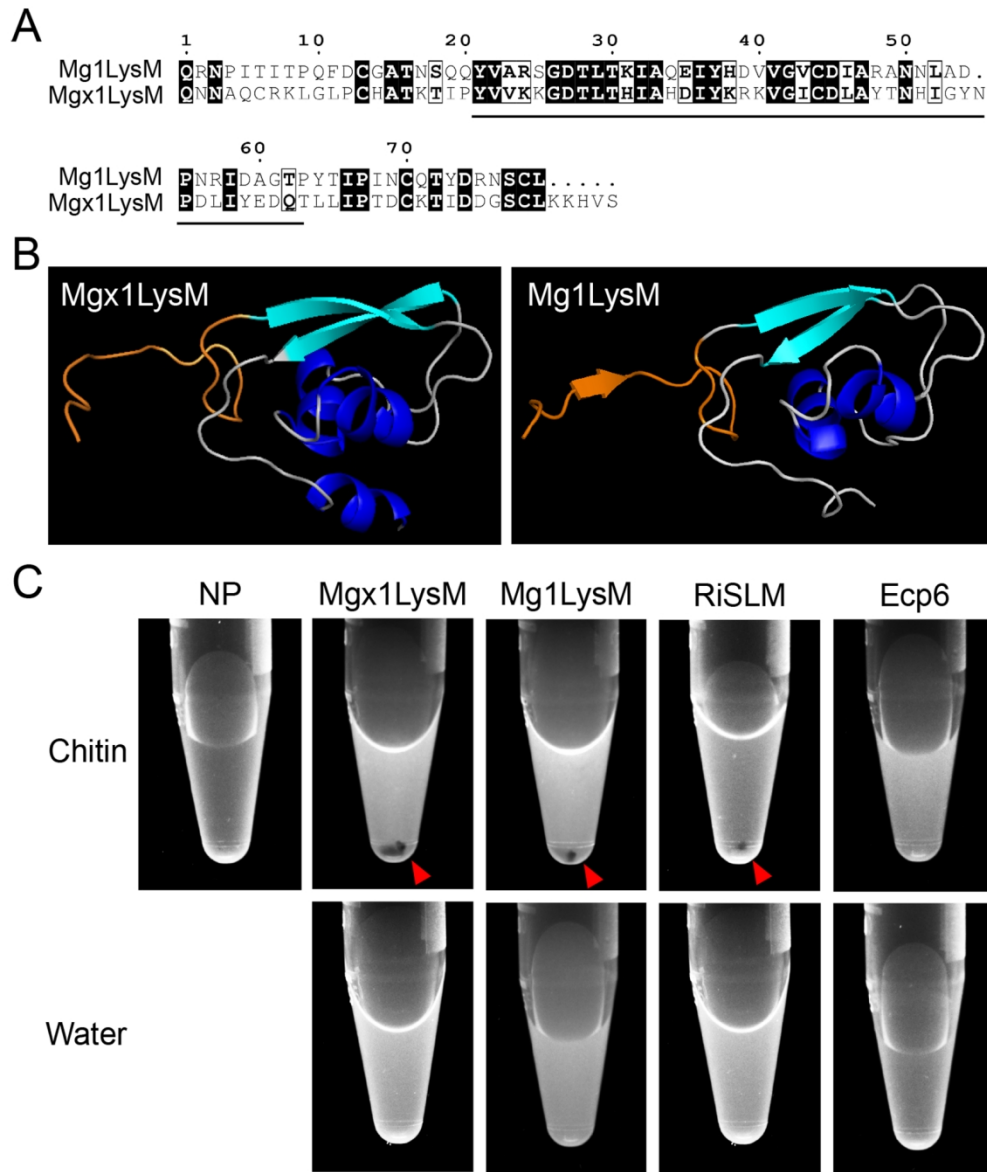
Fig. 6 Mgx1LysM undergoes chitin-induced polymerization. (A) Amino acid sequence alignment of Mgx1LysM and Mg1LysM. The LysM is indicated with black underlining. (B) I-TASSER software-based in-silico prediction of the three-dimensional structure of Mgx1LysM (left) based on the recently generated crystal structure of Mg1LysM (right) (Sánchez-Vallet et al., 2020). The N-terminal 15 amino acids of both proteins are depicted in orange. Structures are visualized using the PyMOL molecular graphics system (Schrodinger LLC, 2015). (C) The LysM effector Mgx1LysM, together with RiSLM and Mg1LysM as positive controls, and Ecp6 as negative control, were incubated with chitohexaose (chitin) or water. After overnight incubation, methylene blue was added and protein solutions were centrifuged, resulting in protein pellets (red arrowheads) as a consequence of polymerization for Mgx1LysM, Mg1LysM and RiSLM, but not for Ecp6.